Materials Horizons

ROYAL SOCIETY OF CHEMISTRY

COMMUNICATION

View Article Online
View Journal | View Issue

Cite this: *Mater. Horiz.*, 2025, **12**, 7425

Received 14th May 2025,
Accepted 11th June 2025

DOI: 10.1039/d5mh00915d

rsc.li/materials-horizons

Ultrasoft, elastic, and ionically conductive polyethylene glycol/ionic liquid bottlebrush ionogels†

Pengfei Xu,[a] Siddhartha Challa,[a] Zefang Zhang,[a] Xia Wu,[a] Shaojia Wang,[a] Peng Pan*[a] and Xinyu Liu*[ab]

Ultrasoft conductors have advanced the field of electronics by achieving a level of softness comparable to that of biological tissues. However, the inherent difference in charge carriers between conventional ultrasoft electronics (utilizing electrons) and tissues (utilizing ions) could lead to high contact impedance, hindering electronic performance for physiological signal recordings. Although ultrasoft hydrogels exhibit ionic conductivity, their high water content could limit their practical applications. This study proposes a type of ultrasoft and ionically conductive bottlebrush ionogel (BBI), leveraging polyethylene glycol (PEG) bottlebrushes and ionic liquids (ILs). The incorporation of ILs into PEG bottlebrushes results in a simultaneous enhancement of mechanical compliance and ionic conductivity. Specifically, the PEG/IL BBI achieves a Young's modulus of 0.52–1.08 kPa, akin to the softest biological tissues such as the brain. To the best of our knowledge, this is the softest ionic conductor ever reported. The introduction of ionic liquids enables ionic conductivity of 0.03–0.29 S m^{-1}, rendering it well-suited for integration into ultrasoft electronics. The PEG/IL BBI was further applied as a sensor on silkworms and as an electrode on the human body and venus flytrap. These demonstrations enabled the sensing of subtle deformations, electrocardiogram recordings, and plant signal monitoring, showcasing the potential of this ionically conductive BBI in various physiological environments.

New concepts

Tissues like the brain exhibit ultra-softness (Young's modulus: ~1 kPa) and transmit electrophysiological signals *via* ions. Electronic materials intended to interface with such tissues must replicate these properties—tissue-matched softness and ionic conductivity. This study introduces an ultrasoft and ionically conductive bottlebrush ionogel (BBI) based on polyethylene glycol (PEG) bottlebrushes and ionic liquids (ILs), achieving a record-low Young's modulus of 0.52–1.08 kPa and a tissue-matched ionic conductivity. Unlike conventional ultrasoft conductors, such as conductive bottlebrush elastomers that rely on electron-based conduction, or ionic hydrogels with high water content, the PEG/IL BBI employs non-volatile ILs. This design not only mimics the ionic charge carriers of biological tissues to enhance signal transmission for bio-interfacing but also addresses stability issues by avoiding water-dependent systems. The PEG/IL BBI was demonstrated in wearable electronics for silkworms and electrodes for monitoring signals in plants and humans, showcasing its bio-interfacing potential. The PEG/IL BBI offers new insights into the development of ultrasoft materials and electronics, expanding the possibilities for soft, stable, and high-performance physiological sensing and bioelectronic interfaces.

1 Introduction

Recent advances in soft electronics have highlighted their broad potential for applications in understanding and interfacing with biological systems.[1,2] To ensure effective integration, it is important to minimize immunological rejections and improve the tissue compatibility of soft electronics used in biological systems.[3] One prominent approach is to match the softness of electronics with those of biological tissues. Ultrasoft electronics are a new type of soft and stretchable electronics that aim to seamlessly interface with biological tissues through matched softness.[4–7] To achieve this, the underpinning materials employed in ultrasoft electronics must possess a Young's modulus akin to that of ultrasoft biological tissues (*i.e.*, Young's modulus, $E < 5$ kPa[8]) and also exhibit suitable conductivities for efficient transmission of electrical signals. For instance, ultrasoft hydrogel conductors have found wide applications in soft actuators,[9] robotics,[10] and implantable devices[11–15] due to their low modulus and tunable conductivities, while the high water content in hydrogels could lead to issues such as dehydration[16] and decomposition during operations,[17] limiting their practical use. Recently, conductive bottlebrush elastomers (BBEs) have

[a] *Department of Mechanical and Industrial Engineering, University of Toronto, Toronto, Ontario, M5S 3G8, Canada. E-mail: peng.pan@mail.utoronto.ca, xyliu@mie.utoronto.ca*
[b] *Institute of Biomedical Engineering, University of Toronto, Toronto, Ontario, M5S 3G9, Canada*

† Electronic supplementary information (ESI) available. See DOI: https://doi.org/10.1039/d5mh00915d

emerged as a new class of ultrasoft conductors.[6,18] The elongated bottlebrush-like side chains in the BBEs can effectively reduce the physical entanglements of polymers and thus a tissue-matched Young's modulus without the need for solvents is achieved.[19–24] By virtue of the ultra-softness of the BBE matrix, ultrasoft conductors can be realized by incorporating conductive components into BBEs. For example, polydimethylsiloxane (PDMS)-based BBEs filled with single-walled carbon nanotubes (SWCNTs) can achieve a Young's modulus as low as 2.98 kPa.[6] However, a notable limitation of current conductive BBEs is that their charge carriers are all based on electrons,[6,18] as opposed to biological systems that primarily rely on ions.[25] Matching the type of charge carriers with those in biological systems can reduce the contact impedance at the interface between electronics and biological systems[26] and enhance the efficiency of signal transmission.[27,28] Thus, an ionically conductive BBE is in demand to build next-generation ultrasoft electronics.

To render the ionic conductivity of BBEs, mobile ion species need to be introduced into the BBE matrix. Common ions in biological systems, such as sodium ions (Na^+), chloride ions (Cl^-) and hydrogen ions (H^+), usually require solvents (*e.g.*, water) to facilitate mobility at room temperature,[29] while the evaporation of such solvents poses stability challenges for long-term electronic use.[30] Another approach is to use salts with low melting points, such as ionic liquids (ILs).[31] Many ILs exhibit low vapor pressure and can be maintained in the liquid state at room temperature.[32] Moreover, ILs have a much wider electrochemical window compared to water,[33] making them promising candidates to be employed in soft electronics. Although the use of ILs has shown advantages in linear elastomers in terms of good ionic conductivity and air stability,[34–36] their Young's modulus still tends to exceed that of ultrasoft tissues (*e.g.*, tissues in brains and lungs can be as soft as 1 kPa), partially due to the high-moduli linear elastomer matrix that was employed.

Here we report an ultrasoft and ionically conductive bottlebrush ionogel (BBI) based on PEG BBEs and IL 1-ethyl-3-methylimidazolium trifluoromethanesulfonate ([EMIM][OTF]). It was found that (i) incorporating a bottlebrush polymer-based ionogel significantly enhanced the matrix softness compared to its linear polymer-based counterparts and (ii) increasing amounts of ionic liquids into PEG-based bottlebrush elastomers (BBEs) simultaneously enhanced their conductivity and softness (resulting in materials with higher compliance) (Fig. 1(a)). The PEG/IL BBI exhibits a Young's modulus as low as 0.52 kPa, surpassing the softness of ionically conductive water-free elastomers previously reported in the literature and achieving the level of softest biological tissues such as the brain. Moreover, this is also the softest water-free conductor ever reported among electronically or/and ionically conductive elastomers. The impressive softness of the PEG/IL BBI is complemented by its tissue-matched ionic conductivity, surpassing 0.03 S m^{-1} attributed to the presence of mobile ion species within the ionic liquids. We apply the PEG/IL BBI as ultrasoft electronics and showcase their demonstrations of capabilities in wearable electronics for silkworms, as well as in physiological signal recording electrodes for the human body and Venus flytrap.

2 Results and discussion

2.1. Design of ultrasoft PEG/IL BBIs

We hypothesize that (i) incorporating a bottlebrush polymer structure will enhance the matrix softness compared to linear polymer networks and (ii) increasing the concentration of ionic liquid within the PEG-based bottlebrush elastomer (PEG BBE) will simultaneously improve ionic conductivity and further soften the network. These two aspects address distinct but complementary mechanisms for tuning ionogel properties. First, regarding polymer architecture, while existing ionogels offer versatile tunability in mechanical properties, achieving an ultralow Young's modulus comparable to that of extremely soft biological tissues, such as the brain (E: ~1 kPa), has rarely been demonstrated. This limitation is likely attributed to the highly entangled polymer networks commonly present in existing ionogels, which restrict overall softness. One strategy to overcome this is to tailor the polymer architecture to reduce the polymer entanglements. By increasing the length of polymer side chains, the polymer backbones can be effectively extended, thereby reducing chain entanglements (Fig. 1(a)). As a result, the bottlebrush architecture with the elongated side chains provides a much softer matrix, making it particularly suitable for the development of ultrasoft ionogels. Second, from the perspective of conductive filler selection, we propose that ionic liquids can serve a dual function. Compared to solid conductive components such as carbon-based or metallic nanomaterials (*e.g.*, carbon nanotubes) that can enhance the Young's modulus of BBE,[6] ionic liquids can decrease the Young's modulus when enhancing the conductivity for materials, due to their capability of swelling the polymer network. As depicted in Fig. 1(a), the ionic liquids can be viewed as non-volatile solvents that swell the PEG BBEs. An increased amount of ionic liquids results in a higher swelling ratio, ultimately rendering the BBI even softer. Simultaneously, a greater amount of ionic liquids introduces more mobile ion species, facilitating the transmission of electrical signals and thereby enhancing the BBI's conductivity.

The architecture of polymers, including factors such as the length of polymer side chains, the spacing between side chains, and the distance between crosslinks, is pivotal in determining the mechanical properties of pure BBEs.[19] To investigate how the bottlebrush structure contributes to the ultra-softness of our materials, we selected methacrylate-based monomers with different ethylene glycol chain lengths to investigate their effect on material properties. Specifically, we used ethylene glycol methyl ether methacrylate (M_n = 144) and poly(ethylene glycol)-methyl ether methacrylate with M_n = 300 and 500 (Fig. 1(a) and (b)), respectively. These correspond to ethylene glycol repeating units (denoted as m in Fig. 1(b)) of approximately 1, 5, and 9, respectively. For simplicity, we refer to these monomers as EG-1, PEG-5, and PEG-9. Poly(ethylene glycol)diacrylate (PEGDMA) with 14 ethylene glycol repeating units was used as the crosslinker. Ethylene glycol-based monomers were chosen for their polarity, which is

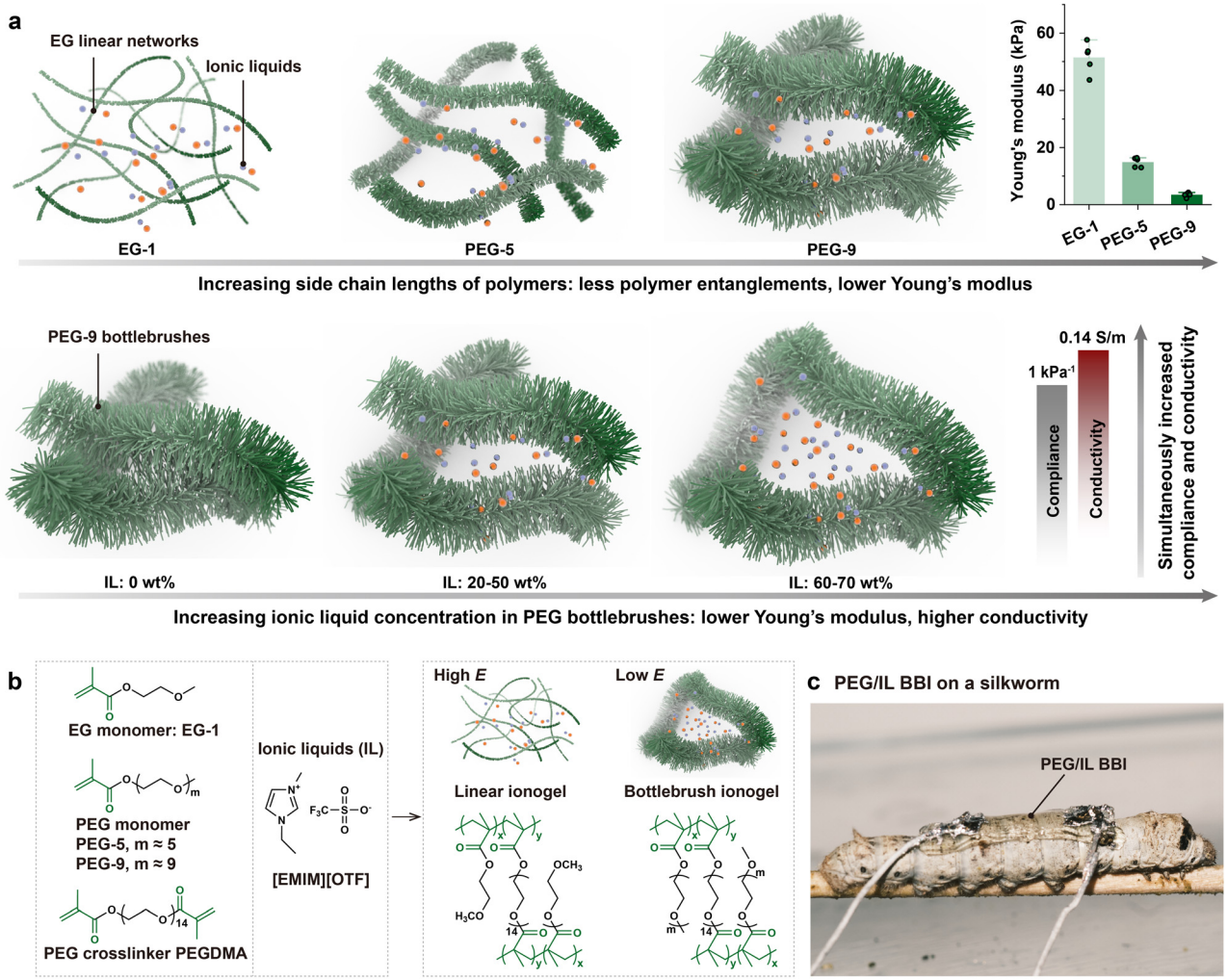

Fig. 1 Design of ultrasoft and ionically conductive PEG/IL BBEs. (a) The top schematic shows ionogels prepared from monomers with different chain lengths, including EG-1, PEG-5, and PEG-9. Increasing the chain lengths leads to a reduction in Young's modulus. The bottom schematic shows PEG BBE (IL: 0 wt%) and PEG/IL BBI with IL contents ranging from 20 to 70 wt%. The compliance and conductivity can be simultaneously enhanced with the addition of ionic liquids. The dimensions in schematics are not to scale. (b) Chemical structures of EG monomers, PEG monomers, PEG crosslinkers, ionic liquids [EMIM][OTF], and the resulting crosslinked linear ionogels and bottlebrush ionogels. (c) A photograph of a piece of PEG/IL BBI attached to the back of the silkworm.

compatible with that of ionic liquids,[37] ensuring good miscibility. In contrast, PDMS-based BBE precursors are less polar and therefore do not blend as readily (Fig. S1, ESI†). Polymerization of these monomers with varying chain lengths results in polymers with correspondingly different side chain lengths. For instance, EG-1, with its short side chains, forms a linear polymer network, while PEG-9 enables the formation of bottlebrush polymer structures, which are the focus of this study. Although PEG monomers with higher molecular weight could result in longer side chains for bottlebrush polymers, they tend to crystallize and affect the mechanical properties after crosslinking.[38] To standardize the initial crosslinking density across samples, we established a fixed crosslinking ratio (molar ratio of monomer to crosslinker) of 1000 to determine the distance between crosslinks. Therefore, the *x*/*y* ratio of bottlebrush elastomer networks shown in Fig. 1(b) was initially designed to be 1000. This design enables us to systematically investigate the effects of side chain length and ionic liquid content on the mechanical properties of PEG-based BBIs.

Ionic liquids [EMIM][OTF] were chosen due to their low melting point (−25.7 °C),[39] wide electrochemical window (3.2 V),[40] and relatively low cytotoxicity.[41] Similar to our previous work on PDMS BBEs,[6] we adopt a one-pot free-radical polymerization method to prepare the ionically conductive linear ionogels and BBIs. The process began with blending monomers having varying side chain lengths with the crosslinker PEGDMA and the thermal initiator azobisisobutyronitrile (AIBN) to form the elastomer precursor. Then the ionic liquid was added to this mixture, and the resulting blend was thermally cured to produce ionically conductive linear ionogels and BBIs. This method offers simplicity for the preparation of BBIs, as all the starting materials are commercially available, sparing us the complexity of chemical synthesis. The straightforward and simple process of preparing BBEs allows us to easily fine-tune their mechanical properties and render the ionic conductivity. Alternative strategies include the synthesis of charged bottlebrush poly(ionic liquids),[42] or the copolymerization of polymerizable ionic

liquids monomers with neutral bottlebrush polymers,[43,44] while these alternatives often entail intricate synthesis and crosslinking of bottlebrush polymers,[45] potentially impeding their practical use for non-chemists. Our approach leads to the creation of a BBE-based ionogel (*i.e.*, BBI) (Fig. 1(c)) that is anticipated to exhibit ultrasoftness and ionic conductivity.

2.2. Characterization of ultrasoft PEG/IL BBIs

To validate our hypothesis, we first prepared ionogels with varying polymer side chain lengths using EG-1, PEG-5, and PEG-9 as monomers. The concentration of ionic liquids was fixed at 50 wt%, resulting in a 1 : 1 weight ratio between the elastomer precursor and the ionic liquid. Upon crosslinking, monomers with longer chain lengths (*e.g.*, PEG-9) formed polymers with longer side chains, yielding bottlebrush elastomers (Fig. 1(a) and (b)). In contrast, low-molecular-weight monomers (*e.g.*, EG-1) produced linear elastomers with short side chains. This variation in side chain length allowed us to investigate how the side chain length affects the mechanical softness of ionogels under a constant ionic liquid content. As a control, we also prepared ionogels using only PEGDMA (without any additional monomer), while maintaining the same ionic liquid concentration. The results show that increasing side chain length leads to a substantial decrease in Young's modulus (Fig. 2(a)), which is attributed to reduced physical entanglements due to the extended side chains. The ionogel composed solely of PEGDMA exhibited the highest modulus, due to its high crosslinking density. Notably, only ionogels with bottlebrush polymer structures achieved a Young's modulus of 3.43 kPa within the ultrasoft tissue range (*i.e.*, <5 kPa) at this ionic liquid concentration. These findings highlight the critical role of bottlebrush polymer architecture in achieving ultra-low modulus in ionogels. Therefore, to maintain the bottlebrush polymer structure, in all subsequent experiments, the materials were prepared using PEG-9 as the BBE monomer to form PEG/IL BBIs.

To further enhance the softness of the BBIs and achieve a Young's modulus that is comparable to ultrasoft tissues such as the brain (*E*: ~1 kPa), we then adjusted the amount of added ionic liquids. We tested five different weight ratios of PEG BBE precursors to ionic liquid: 1 : 0, 1 : 0.25, 1 : 0.5, 1 : 1, and 1 : 1.5. These correspond to ionic liquid concentrations of 0 wt%, 20 wt%, 33 wt%, 50 wt%, and 60 wt%, respectively. The fitting model for bottlebrush elastomers was adapted to fit the σ_{true}–strain curve (Fig. S2, ESI†) and calculate the fitted Young's modulus (*E*) of materials (see details in Table S1, ESI†). The engineering Young's modulus (E_{eng}) can be obtained by fitting

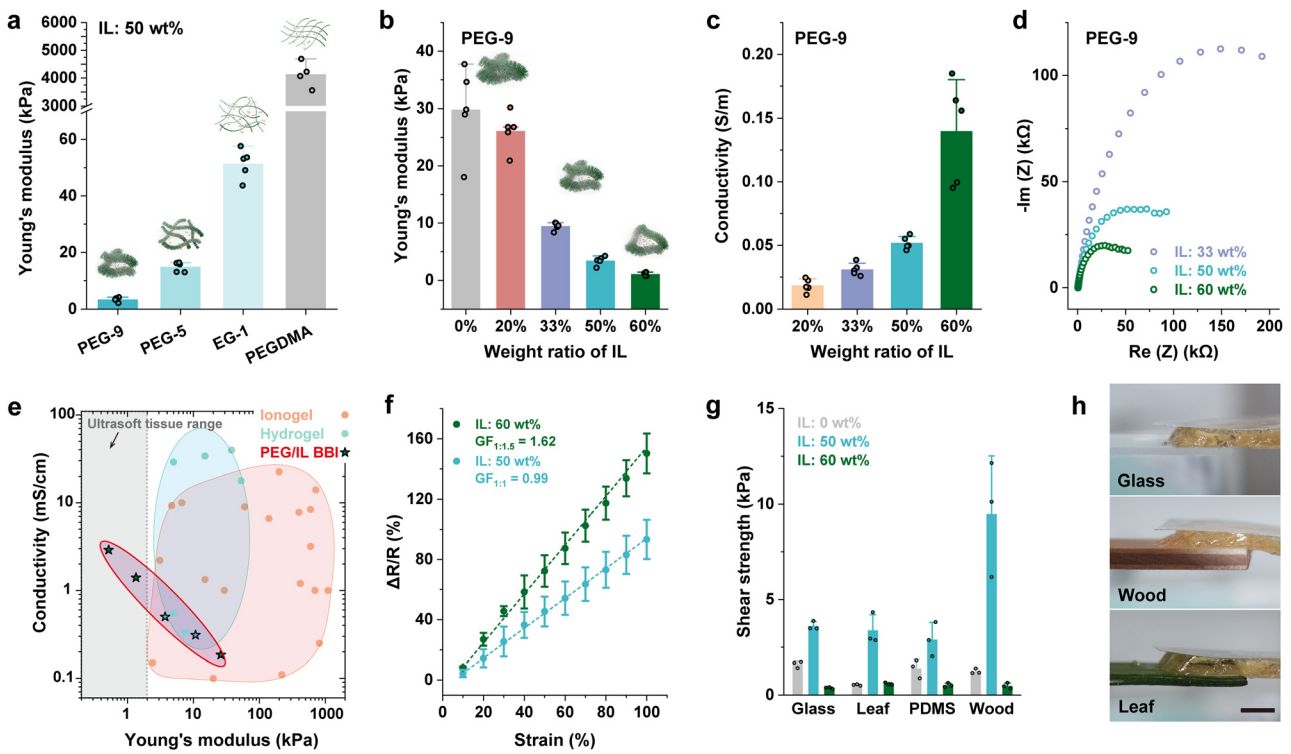

Fig. 2 Characterization of PEG/IL BBIs. (a) The Young's modulus of ionogels prepared from monomers with different chain lengths shows that looser crosslinking and longer polymer side chains enhance the softness. (b) The reduced Young's modulus and (c) enhanced conductivity of PEG/IL BBIs with the addition of ionic liquids. (d) The real and imaginary impedance of PEG/IL BBI with different concentrations of ionic liquids measured at the frequency ranging from 10 000 Hz to 0.1 Hz. (e) The Ashby-style plot of Young's modulus and conductivity of different ionic conductive elastomers including ionogels, hydrogels, and PEG/IL BBIs in this work, showing our PEG/IL BBI (IL: 60–70 wt%) is the softest ionically conductive elastomer in the graph. Data points are from references labelled in Fig. S9 and Table S2 (ESI†). (f) The sensitivity of PEG/IL BBIs measured as normalized change in resistance as a function of tensile strain. (g) The adhesive shear strength between the PEG/IL BBI (IL: 50 wt% and 60 wt%) and different substrates, including glass, leaf, PDMS Sylgard 184, and wood. (h) Photographs of the adhesion test between the PEG/IL BBI and different substrates showing the adhesion-induced deformation of BBIs. The scale bar is 5 mm.

the nominal stress–strain curve at the strain range of 0–10% and are summarized in Table S1 (ESI†). The Young's modulus calculated by the two methods exhibited similar levels, and the fitted Young's modulus was used for analysis. The pure PEG BBE exhibits a Young's modulus of average E: 29.84 kPa when no ionic liquids were introduced (Fig. 2(b)). Increasing the weight ratio of ionic liquids from 0% to 20%, 33%, and 50% led to a corresponding decrease in Young's modulus from 29.84 kPa to 26.11 kPa, 9.46 kPa, and 3.43 kPa, respectively. The modest reduction at 20% suggests that the small amount of ILs did not significantly swell the elastomer matrix. Therefore, we focused our evaluation on higher IL concentrations. At higher weight ratios, the additional IL content caused greater swelling of the polymer network, substantially softening the PEG/IL BBI material. For instance, at 60 wt% IL, the Young's modulus further decreased to an average of 1.08 kPa (Fig. 2(b)), corresponding to the softness level found in brain tissues.[8] In addition to the swelling effect, the significant reduction in Young's modulus after the addition of ionic liquids indicates a decrease in crosslink density, enabling our materials to achieve a more than ten-fold decrease of Young's modulus with a swelling ratio of less than two (*e.g.*, at an IL content of 50 wt%). The incorporation of ionic liquids could markedly reduce the crosslink density and affect the effectiveness of gelation,[46,47] which is possibly attributed to solvent effects such as the polarity difference between the monomers and ionic liquids.

To investigate the lowest Young's modulus achievable through the incorporation of ionic liquids into the bottlebrush architecture, we have also prepared EG-1 ionogels and PEG-9 ionogels (*i.e.*, BBIs) with even higher concentrations of ionic liquids. The maximum achievable IL loading to ensure effective gelation was 70 wt%. We measured the Young's modulus and conductivity of both the EG-1 ionogel and the PEG-9 BBI at 70 wt% IL loading (Fig. S3, ESI†). Their conductivities were comparable due to the same concentration of ionic species. However, the mechanical properties differed significantly. The EG-1 ionogel exhibited a Young's modulus of approximately 1 kPa, whereas the PEG-9 BBI achieved a much lower modulus of 0.52 kPa. This result supports our key finding: the bottlebrush architecture consistently enables a lower Young's modulus than the linear counterpart. With the same IL content, bottlebrush-based ionogels are significantly softer than those derived from linear gels. Similarly, to achieve the same level of ultra-softness, bottlebrush ionogels require substantially less ILs than linear ionogels. While high IL loading can also reduce the modulus of linear ionogels, our results indicate a clear limit—1 kPa appears to be the lowest modulus achievable with linear structures in our system. In contrast, bottlebrush ionogels can readily achieve a modulus around 0.5 kPa, a range that matches those of some supersoft tissues such as the extracellular matrix and adipose tissue.[48,49] These findings underscore the unique advantages of the bottlebrush architecture in applications where conventional linear structures fall short.

It should be noted that not all liquid-phase ionic liquids are effective in swelling and softening the bottlebrush elastomer network. For instance, we also synthesized reactive ionic liquids, which contain vinyl or acrylate groups that enable them to participate in polymerization. Specifically, we designed two types of reactive ionic liquids, [2-(methacryloyloxy)ethyl]trimethylammonium bis(trifluoromethylsulfonyl)imide ([METAC][TFSI], MT) and 1-ethyl-3-methyl imidazolium (3-sulfopropyl) acrylate ([EMIM][SPA], ES), with mobile cations and anions, respectively (Fig. S4, ESI†). By copolymerizing these reactive ionic liquids with PEG-based BBE monomers, we formed a co-polymerized network comprising both PEG and ionic liquid components. However, the resulting ionogels exhibited significantly higher Young's modulus, 61.06 kPa for ES and 25.78 kPa for MT, compared to the PEG-based BBI (Fig. S5, ESI†). This outcome is expected, as the copolymerization of ionic liquids with PEG reduces the density of PEG side chains. This reduction can increase the degree of physical entanglements within the network, thereby increasing the Young's modulus.[19,50] Therefore, material selection should be guided by the specific property requirements of the design. In our case, since we aimed to achieve an ultra-softness, we selected the PEG/IL BBI, as our experiments demonstrated that it was the only formulation capable of reaching the ultralow Young's modulus ($\sim$1 kPa).

Previous studies have shown that the lightly crosslinked polymer strands and fewer polymer entanglements in BBEs can enhance the stretchability and elasticity of elastomers,[6] which aligns with our findings for PEG/IL BBIs. We conducted cyclic tensile testing at a 100% strain with a fixed strain rate of 0.07 s^{-1} (rate of deformation: 50 mm min^{-1}). All BBIs and the pure BBE with different loading amounts of ionic liquids exhibited a fully reversible deformation and minimal hysteresis (Fig. S2 and Fig. S6, ESI†), indicating their good elasticity and stretchability. The reversible deformation (Fig. S6, ESI†) in the repeated loading–unloading cycles of samples further indicates the durability of materials. It should be noted that compared to pure PEG BBE, BBI with a higher weight ratio of ionic liquids (IL concentration: 60 wt%) exhibited a larger hysteresis in the loading–unloading cycle (Fig. S6, ESI†) and a more noticeable frequency-dependent storage modulus (Fig. S7, ESI†), indicating the viscoelastic behaviour of the PEG/IL BBI. This is possibly attributed to the addition of ionic liquids that affected the relaxation process of the bottlebrush networks.[51,52]

Previous investigations into conductive BBEs grappled with the challenge of balancing conductivity and softness.[6,53] This challenge was primarily due to the propensity of conductive fillers to elevate Young's modulus of the BBE composites.[54] Conventional conductive fillers, such as carbon nanotubes and silver nanowires, are non-thermal and act as reinforcing agents that promote solid-like behavior, often at the expense of softness. In contrast, ionic conductors like free ions are typically thermal, with higher mobility than the polymer matrix. This allows them to act as plasticizers, softening the material instead of stiffening it. We found that the ionic liquids can not only soften the BBE network but also enhance the conductivity of the BBEs. We used the four-point probe measurement to test the conductivity of the PEG/IL BBIs with different amounts of ionic liquids. At weight ratios of 20%, 33%, 50%, 60%, and 70%, the electrical conductivities of the PEG/IL BBIs were measured to be 0.02 S m^{-1}, 0.03 S m^{-1}, 0.05 S m^{-1},

0.14 S m^{-1}, and 0.29 S m^{-1} (Fig. 2(c) and Fig. S3b, ESI†), respectively. Compared to pure BBEs without any ionic liquids, PEG/IL BBIs are significantly softer and more conductive. However, the ionic conductivity is still lower than that of pure ionic liquids [EMIM][OTF] ($\sim$0.92 S m^{-1}), as the highest concentration we added was 70 wt% and the ionic mobility could be limited by the nonconductive PEG segments. The BBI with 70 wt% IL was found to be extremely soft and challenging to handle. Therefore, in all subsequent experiments, we limited the maximum IL concentration to 60 wt% to ensure better processability and material stability. Next, we used electrochemical impedance spectroscopy (EIS) to assess the impedance of PEG/IL BBIs by sweeping the frequency from 10^5 Hz to 0.1 Hz. For PEG/IL BBIs with different weight ratios of ionic liquids, the impedance is dependent on the applied frequency (Fig. S8, ESI†), and the Nyquist plot displays a semi-circle pattern (Fig. 2(d)), indicating the capacitance derived from the mobile ion species within the PEG/IL BBIs.[55] Moreover, a higher weight ratio of ionic liquids leads to a lower impedance across the frequency spectrum, which is attributed to an increased volume of ion species that enhanced the overall charge mobility. The results from EIS affirm that incorporating ionic liquids can improve the ionic conductivity of the PEG/IL BBIs. We compared our materials with other types of ionically conductive materials, including hydrogels and iongels. The Ashby-style plot in Fig. 2(e) shows that our PEG/IL BBIs are softer than most ionically conductive hydrogels and ionogels. At the weight ratio of 60–70%, our PEG/IL BBI stands out as the softest ionic conductor among all the ionically conductive materials ever reported (Fig. S9 and Table S2, ESI†), falling within the ultrasoft tissue range. The PEG/IL BBI is also softer than our previously reported SWCNT/PDMS BBE, making it the softest conductive and water-free bottlebrush materials ever reported. One of the closest competitors to BBIs in terms of softness is hydrogels, particularly bottlebrush hydrogels,[56–58] which are another promising class of materials with tissue-matching mechanical properties. While the ionic conductivity of bottlebrush hydrogels has not been extensively studied, they hold strong potential for tuning toward ionic transport. However, a key limitation of hydrogels lies in their high water content, which can lead to mechanical and electrical instability due to dehydration, especially in open-air environments. In contrast, the PEG/IL BBI exhibits superior long-term stability in both mechanical properties and conductivity (Fig. S10, ESI†), owing to the low volatility of ionic liquids. This environmental robustness offers a distinct advantage for practical applications, particularly in soft electronics that operate under ambient conditions. However, intrinsic limitations of ionic liquids—such as leaching and swelling in wet conditions and evaporation at high temperatures—pose challenges for deployment in more demanding environments. To address these issues, future studies will focus on developing more robust materials and device architectures. For example, designing highly reliable polymers or applying non-leaching, dry insulating materials for encapsulating the ionogels can be effective strategies to meet specific application requirements.

The ionic conductivity and stretchability endow mechanical sensitivity for the PEG/IL BBIs. The resistance change of the PEG/IL BBIs was recorded when stretching them to different strains (ranging from 0 to 100%). The normalized change of resistance exhibits a linear correlation with the applied strain. At weight ratios of 50% and 60%, the gauge factors are 0.99 and 1.62, respectively (Fig. 2(f)). The higher gauge factor at the weight ratio of 60% suggests enhanced sensitivity. This is possibly because higher loading of ionic liquids provides an increased quantity of charged carriers within the system, and thus more charge carriers are redistributed during stretching. Although only strain sensing was demonstrated in this work, the material also shows potential for use as a pressure sensor. Since the IL concentration influences both the ionic conductivity and the Young's modulus, these two factors jointly determine the material's sensitivity in different sensing modes. This mechanical sensitivity could be useful in applications where matching the softness of biological tissue is critical, offering an advantage over conventional sensors that may not achieve the same level of mechanical compliance. While the ultralow Young's modulus of the material suggests the potential for detecting small forces or deformations, achieving optimal sensitivity may still require further design improvements, such as adjusting the device structure and refining the electrode materials, to enhance overall sensor performance.

In our prior study, we found that the BBEs possess satisfactory interfacial adhesion with diverse material surfaces, a characteristic stemming from their ultra-softness which maximizes contact surfaces and ensures conformity when interfacing with different substrates.[6] Extending this observation to our PEG/IL BBIs, we conducted the same lap shear testing on surfaces of glass, PDMS, leaf, and wood (Fig. 2(g) and (h)). For pure PEG BBE with no ionic liquids added (weight ratio of 0%), the average shear strength was 1.61 kPa, 0.53 kPa, 1.39 kPa, and 1.24 kPa, respectively. However, at a weight ratio of 50%, the average shear strength was measured to be 3.61 kPa, 3.38 kPa, 2.90 kPa, and 9.48 kPa, respectively. We hypothesize that this substantial increase in shear strength can be attributed to the addition of ionic liquids that lead to the change of chemical composition[59] or capillary effects[60] of the material system, which enhanced softness and increased contact areas between the BBI and substrates, and thus facilitates better conformity and adhesive properties. It should be noted that at higher concentrations of ionic liquids (weight ratio of 60%), the shear strength declined (Fig. 2(g)). This is because the shear strength is linked to the material's mechanical strength. The PEG/IL BBI at the weight ratio of 60% is already ultrasoft (with a Young's modulus of $\sim$1 kPa and stress at 100% strain of $\sim$1 kPa), and the BBI could potentially rupture when the shear strength surpasses the stress tolerance of the BBI (Fig. S11, ESI†). Overall, these results show the material's capability of adhering to hydrophobic surfaces and the potential of using it as gentle, wearable electronics for delicate objects such as plants. Although this level of shear strength may seem relatively low when compared to traditional adhesive materials, the PEG/IL BBIs displayed considerable deformation in the lap shear

testing (Fig. 2(h)). Furthermore, the PEG/IL BBI can easily attach to skin without detaching, and this level of adhesion can withstand its own gravity and different strain levels during operation (Fig. S12, ESI†). All the results showcase that the PEG/IL BBIs maintain a certain level of adhesion properties that could be beneficial to applications of ultrasoft electronics.

2.3. Wearable electronics for the silkworm

As the demand for understanding biological systems and emulating their behaviours grows, electronics must possess better conformability with biological systems. We believe electronics based on the ultrasoft and conductive PEG/IL BBI could potentially broaden the capabilities of previously utilized soft materials. The low Young's modulus of our PEG/IL BBI aligns with those of biological tissues, reducing mechanical constraints, while the self-adhesive properties facilitate good physical contact with tissues. These features collectively enhance the conformability with ultrasoft objectives. To demonstrate, we designed wearable electronics for silkworms, whose body has a much lower modulus (37.7 kPa[61]) than most of the previously reported soft conductors. We hypothesize that the PEG/IL BBI-based electronics could serve as sensors for monitoring the physical movements of soft-bodied animals due to their matched softness and satisfactory adhesion.

The wearable electronics for the silkworm were made by a strip of the PEG/IL BBI (width: 4.6 mm × length: 37.6 mm), with the two ends coated by the Ag/EGaIn composites to connect with external platinum wires and a source meter. We attached the PEG/IL BBI sensor on the back of a silkworm through its self-adhesive properties (Fig. 3(a)) and recorded the resistance change of the sensor during the worm's crawling. Silkworms move using thoracic legs, anterior legs, and an anal proleg[62,63] (A8–A1 denote their main body segments; Fig. 3(a)). Their crawling cycle begins when the anal proleg (AP) detaches from the wood stick, moves forward, and reattaches. The anterior legs (segments A6–A3) then advance sequentially until the thoracic leg reaches the endpoint, completing the cycle (Fig. 3(b)). We analyzed movement by tracking three key points: the anal proleg (AP), A6, and A3. The cycle starts when the AP lifts off the wood stick and ends just before the AP detaches again for the next cycle. The ultrasoft, adhesive PEG/IL BBI sensor remained securely attached, enabling continuous recording of the silkworm's movements. Wire-induced signal noise was negligible compared to deformation-induced changes (Fig. S13, ESI†). The sensor's resistance exhibited a repeating pattern that matched the silkworm's body contractions and extensions (Fig. 3(c)). Each crawling phase is marked by the silkworm lifting a foot from the substrate. Initially, the silkworm is fully extended, corresponding to the highest sensor resistance. As the worm begins to contract and compress the BBI sensor, the resistance decreases accordingly. The response allows us to pinpoint specific phases of movements (labelled "Start," "A6," "A3,"

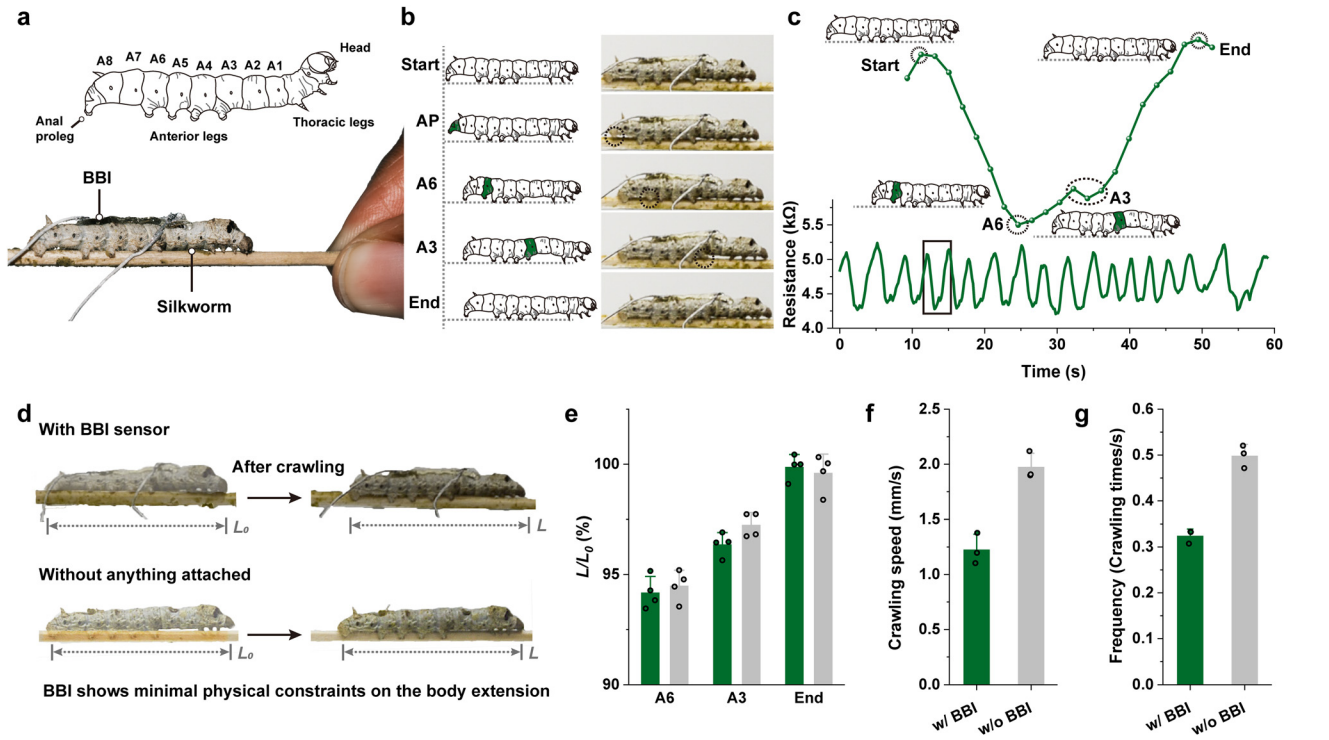

Fig. 3 PEG/IL BBI-based wearable electronics for silkworms. (a) A schematic of the silkworm showing its main body segments and a photograph of the silkworm with the PEG/IL BBI-based wearable electronics. (b) The schematic and photographs of the silkworm moving forward at different crawling steps. (c) The measured resistance of the PEG/IL BBI sensor in response to the worm's crawling movements. (d) Body lengths of the silkworm with and without attaching the BBI sensor show negligible difference after silkworm's crawling. A crawling time of 33 s was recorded. (e) The normalized change in body length of worms, (f) crawling speed, and (g) frequency with and without the BBI sensor attached.

and "End"). This precision in tracking the worm's movement is attributed to the sensitivity of the PEG/IL BBI, resulting in notable resistance changes in response to small movements. Comparing silkworms with and without the PEG/IL BBI, there were no differences in the body extension ratio (the body length at each representative crawling point divided by its initial length) between the two groups of worms (Fig. 3(d) and Movie S1, ESI†). At the crawling points labeled as "A6", "A3", and "End", the corresponding body length remained nearly constant (the worm length was around 95%, 97%, and 100% of its initial length at the three representative points for both cases) (Fig. 3(e)). In the forward moving direction, the BBI reveals no physical constraints to the contraction and extension of body segments due to its matched softness with that of silkworms. From our experiments, we also found that the sensor-wearing worms show a lower crawling speed (forward moving distance in one crawling cycle divided by the time) and frequency (the number of crawling cycles within a specified time frame) than those without attachments (Fig. 3(f) and (g)). We speculate that this is attributed to the added weight of the external platinum wires and BBI sensor, which introduced additional pressure and slowed its movements. Therefore, more deliberate sensor designs, such as ultrathin nanomesh,[64] can be employed to further enhance the sensor's performance. These results underscore the potential of our conductive PEG/IL BBI as ultrasoft wearable electronics and highlight its capabilities in the study of biomechanics[61] and bio-mimicking robotics.[65]

2.4. Ultrasoft electrodes on the human body and venus flytrap

The ionic conductivity of PEG/IL BBI endows the capability of ionic communication with biological systems. Previous reports have demonstrated the potential of ionically conductive hydrogels [*e.g.*, adhesive poly(acrylic acid) hydrogels] in applications involving signal conduction in biological systems,[66] but the issue of dehydration raises concern for their long-term use. We hypothesize that the ionic conductivity of our water-free PEG/IL BBI could ensure compatibility between its charge carriers (ions) and those of biological systems, while the ultra-softness of the material enhances its adhesiveness, enabling it to conform to various surfaces and effectively record bio-signals, and even stimulate local response in biological systems. To demonstrate, we first compared the roles of ionic and electronic conductivity in physiological signal recording by conducting impedance measurements using both BBI-based electrodes and our previous CNT-based BBE electrodes[6] of the same dimensions on human skin. The CNT BBE electrodes conduct electricity *via* electrons as charge carriers. The impedance spectrum shows that at 1 kHz, the impedance measured with ionically conductive BBI electrodes is significantly lower than that of the electronically conductive BBE electrodes (Fig. 4(a) and Fig. S14, ESI†). This reduced impedance is also observed when the electrodes are applied to plants. This outcome is expected, as BBI shares the same type of charge carriers (ions) with human skin, thereby reducing the contact impedance. In contrast, CNT BBE electrodes rely on electronic conduction, and the mismatch in charge carrier type leads to a relatively higher contact impedance. This demonstrates that the ionic conductivity of our ionogels provides a clear advantage for bio-interfacing applications. Then, we applied the PEG/IL BBI as electrodes on the human body to perform electrocardiogram (ECG) measurements (Fig. 4(b)). We prepared three circular BBI electrodes with a diameter of 8 mm and a thickness of 2 mm by moulding and attached them to the human body as the electrode interface for recording ECG signals. The Ag/EGaIn composite was applied at the top surface of BBI to connect with external platinum wires. These three electrodes were placed at the right arm position (RA), left arm position (LA), and right leg position (RL), respectively. Thanks to the adhesion properties of the PEG/IL BBI, the electrodes can attach with skin conformally, ensuring a good electrical contact during electrophysiological signal recording. The ECG patterns in Fig. 4(c) show that PEG/IL BBI electrodes can successfully record the ECG signals from the human body. We also used the commercial ECG electrode pad with a hydrogel interface to compare its performance with that of PEG/IL BBI electrodes. By comparing with signals recorded by commercial hydrogel electrodes, the PEG/IL BBI electrodes exhibit similar electrical performance. Furthermore, we analysed the signal-to-noise ratio (SNR) of ECG signals from the two types of electrodes. Both types of electrodes perform similar SNR (Fig. 4(d)), indicating that the PEG/IL BBI could serve as an alternative to the commercial hydrogel electrodes, offering advantages such as good ionic conductivity, air stability, and adhesion properties.

In addition to recording electrical signals from the human body, we selected the Venus flytrap as a plant model and used our PEG/IL BBI to modulate its electrophysiology. In contrast to using adhesive hydrogels as the conformal electrodes,[67] we employed the PEG/IL BBI as electrodes as it shares advantages of hydrogels such as high conformability, adhesive properties, and ionic conductivity. Additionally, the water-free PEG/IL BBI may offer better long-term stability than hydrogels. Here, we followed the methodology of previous work,[67] in which two pairs of electrodes were attached to the two lobes of the flytrap respectively (Fig. 4(e) and Movie S2, ESI†). One pair of electrodes was responsible for stimulating the lobes to close, and the other was used to record response signals from the lobe. The conformable electrodes were based on circular PEG/IL BBIs with a diameter of 8 mm, where the Ag/EGaIn composite was applied at the top surface of BBI to connect with external platinum wires, and the bottom surface of BBI made direct contact with the lobe. The distance between the two electrodes on each lobe was fixed at 2 mm. We first applied a direct current (DC) of 4 V to one lobe through the stimulating electrodes, and simultaneously recorded the signal response of the other lobe through the recording electrodes. One can see that the flytrap displays a significant instantaneous spike and a series of action potentials in the recorded signal response upon the application of the DC voltage input (Fig. 4(f)). The lobe closure was induced after the second action potential, and the response time ranges from 6.13 s to 7.17 s, consistent with results in the literature.[67] Next, we varied the stimulating voltage to 2 V, 3 V, and 5 V, respectively. The flytrap displayed two clear action potentials before the closure of lobes, while the

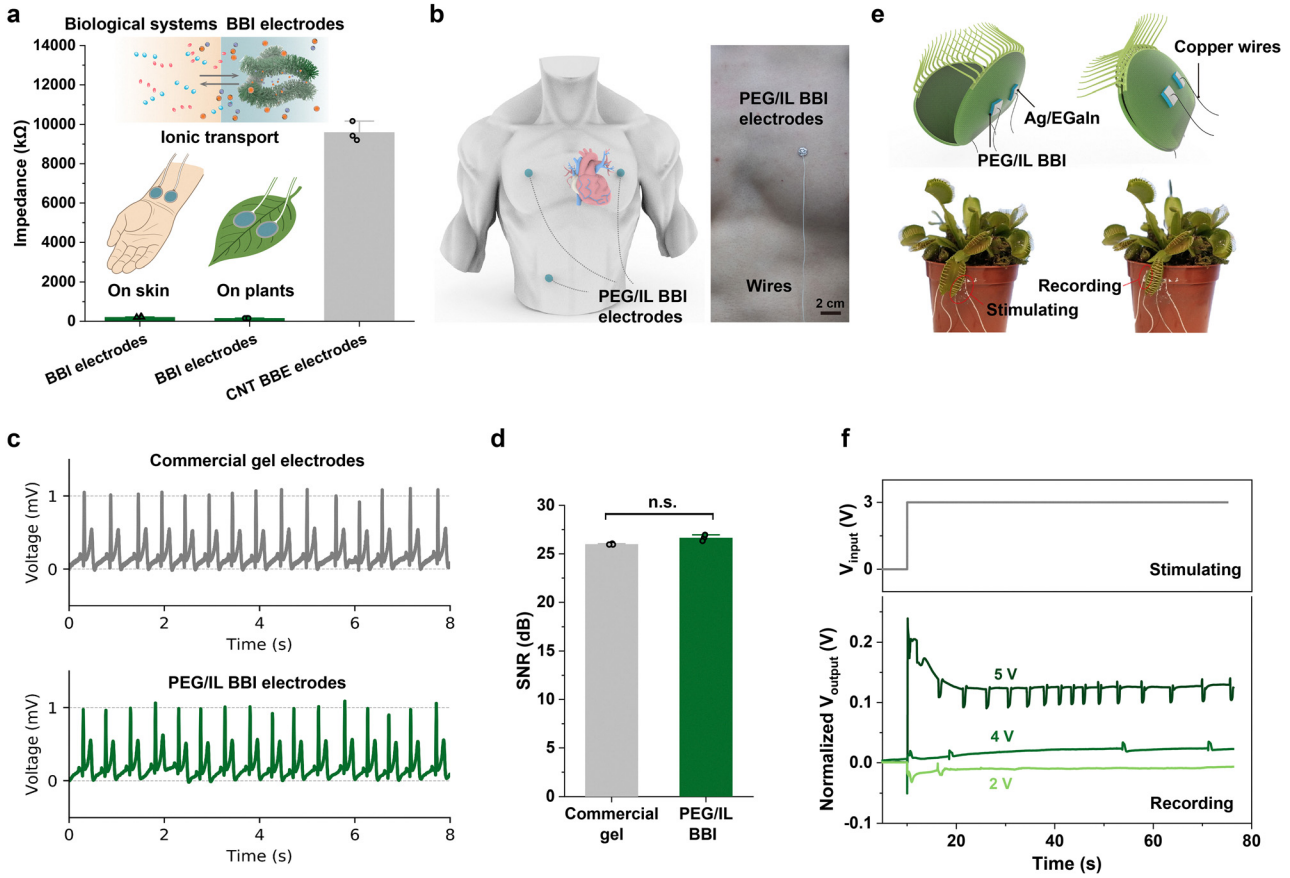

Fig. 4 PEG/IL BBI-based electrodes for the human body and Venus flytrap. (a) Impedance at 1 kHz using BBI (on skin and plants) and BBE electrodes, showing lower impedance for BBI due to the ionic transport at the biology–electrodes interface. (b) Schematic and photograph showing the attachment of the PEG/IL BBI electrodes on the human body. (c) Experimental data of ECG signals measured by commercial gel electrodes and PEG/IL BBI electrodes. (d) The SNR calculated from ECG signals measured by commercial gel electrodes and PEG/IL BBI electrodes showing similar electrical performance. Comparison of SNR from two types of electrodes showing no statistically significant difference (n.s., p = 0.0643). (e) Schematics and photographs showing the lobe closure of the Venus flytrap and attachment of the PEG/IL BBI electrodes. The pair of recording electrodes and pair of stimulating electrodes were attached to the two lobes of the flytrap, respectively. (f) The recorded signal response from the Venus flytrap stimulated by various DC voltage inputs (2 V, 4 V, and 5 V).

frequency of subsequent action potentials reduced at lower voltage inputs (2 V and 3 V) (Fig. 4(f) and Fig. S15, ESI†). This is possibly due to the reduction of the plant tissue conduction at the lower stimulating voltages.[68,69] Then, we transmitted from the DC voltage input to an AC square wave with an amplitude of 4 V and a frequency of 1 Hz (Fig. S16, ESI†). This change resulted in a shortened response time (1.3 s) for the lobe closure (Fig. S17a, ESI†). When the frequency of the AC voltage input increased to 2 Hz, the response time was 1 s (Fig. S17b, ESI†). The rising edge and falling edge in a single square wave can induce two action potentials, which could actuate the closure of the lobes. Thus, an AC voltage input generates the action potential more rapidly than a DC voltage, and as a result, shortens the response time for the lobe closure. It should be noted that the response time is limited by the refractory period of the flytrap ($\sim$1.2 s[67]), so we selected 2 Hz (the corresponding response time is 1 s) as the highest frequency of the input AC voltage. These results highlight the potential of the PEG/IL BBI in bioelectronics demonstrations.

3 Conclusions

We have developed an ionically conductive PEG/IL BBI with ultralow Young's modulus (0.52–1.08 kPa) and ionic conductivity (0.03–0.29 S m^{-1}). The incorporation of ionic liquids into PEG-based BBE can simultaneously reduce the Young's modulus and increase the ionic conductivity of the elastomers. The ultra-softness of the material endows a satisfactory adhesion on various surfaces, rendering PEG/IL BBI ideal for use as interfaces of soft electronics. Meanwhile, the PEG/IL BBI shares the same type of charge carriers (ions) as tissues, allowing it to interact with biological systems through ionic transduction and exhibit potential for bio-interfacing electrodes compared to electronically conductive bottlebrush elastomers (Table S3, ESI†). We prepared PEG/IL BBI-based electronics and demonstrated their capabilities in wearable electronics for soft-bodied worms, as well as in electrophysiological measurements for the human body and plants. Compared to ultrasoft hydrogels, PEG/IL BBIs can achieve a similar level of ultra-softness (*e.g.*, $<$5 kPa) and thus represent a promising alternative, particularly due to their

enhanced stability and resistance to dehydration during fabrication and operation. While ultrasoft hydrogel-based bio-interfacing electronics have shown great potential in interfacing with delicate tissues such as the brain and neurons owing to their excellent biocompatibility,[11,70] PEG/IL BBIs may also be suitable for such applications. In the future, efforts to combine the strengths of both ultrasoft hydrogels and BBIs could further enable the development of multifunctional and high-performance bio-interfacing electronics.

While we presented a material platform for designing ultrasoft electronics, engineering strategies or new material designs need to be developed to enhance its practicality for diverse application scenarios. For instance, the leaching of ionic liquids could be a biocompatibility concern for long-term biological applications. Further development on encapsulating the PEG/IL BBI or designing non-leachable bottlebrush ionic liquids is necessary. In addition, it is still challenging to fully mimic the characteristics of tissues. For instance, current PEG/IL BBIs have limitations in mimicking mechanical behaviours such as strain-hardening characteristics[19,22] or ultimate toughness,[71] which needs new designs of materials and electronic devices. In summary, we introduced a simple and straightforward method to prepare a material capable of achieving unprecedented softness alongside typical ionic conductivity. We explored the material's capabilities across various fields, revealing its distinctive capabilities and potential as bio-interfacing electronics compared to previously reported electronically conductive bottlebrush elastomers. The ultrasoft and ionically conductive PEG/IL BBI presents a promising alternative to many conventional underpinnings of electronics and will expand our capabilities of developing the field of ultrasoft electronics.

4. Methods

4.1. Materials

The monomer poly(ethylene glycol)methyl ether acrylate (447943-500ML, average molecular weight 500 g mol^{-1}), the crosslinker poly(ethylene glycol)diacrylate (PEGDMA, 437468-250ML, average molecular weight 750 g mol^{-1}), and the ionic liquids 1-ethyl-3-methylimidazolium trifluoromethanesulfonate ([EMIM][OTF]) were purchased from Sigma-Aldrich. The thermal-initiator 2,2′-azobis(2-methylpropionitrile) (AIBN, 440190-25G, 98%) was purchased from Sigma-Aldrich and used as received.

4.2. Synthesis of reactive ionic liquids

The synthesis of [METAc][TFSI] was performed by adapting a previously documented synthesis method.[49] In a typical procedure, 7.58 grams (26.40 mmol) of Li[TFSI] was dissolved in 10 mL of deionized water at 70 °C. This solution was then introduced into a vigorously stirred aqueous solution containing 6.25 grams (24.00 mmol) of [METAC]Cl. An excess amount of Li[TFSI] was employed to drive the ion exchange process to completion. Immediately after mixing, two immiscible liquid phases developed. The system was left to stir at room temperature for an additional 4 hours to allow full phase separation. The top aqueous layer was carefully removed, and the remaining ionic liquid phase was thoroughly washed three times with deionized water to eliminate any residual LiCl and unreacted components. The final product was dried using a custom-built column containing magnesium sulfate as a drying agent, yielding a clear, oily, and viscous liquid. The synthesis of [EMIM][SPA] was performed based on a previously reported method[17] with slight modifications. In a typical procedure, 3.15 grams (21.50 mmol) of [EMIM]Cl was mixed with 5.00 grams (21.50 mmol) of K[SPA] in 15 mL of acetonitrile. To inhibit unwanted side reactions, 5 mg of methoxyphenol was added to the mixture, which was then stirred vigorously at ambient temperature overnight. Following the reaction, the formed KCl precipitate was removed by filtration, and the acetonitrile was evaporated under reduced pressure by stirring. The residue was subjected to further vacuum drying at 10^{-1} torr to eliminate any remaining solvent. The resulting oil was dissolved in fresh dichloromethane (DCM) and stored at temperatures below 0 °C overnight to encourage additional salt crystallization, which was then separated by filtration. After final solvent removal, a yellow viscous oil was collected as the end product.

4.3. Preparation of PEG/IL BBIs

PEG monomer (or EG monomers, EG-1), PEG crosslinker PEGDMA, and thermal-initiator (AIBN, 2 mol% of PEG monomers and crosslinkers) were added into a tube. The molar ratio of the monomer and crosslinker was 1000 : 1. The solutions were then mixed by a vortex mixer with a speed of 3000 rpm for 4 minutes and used as the pure elastomer precursor. Next, the pure elastomer precursor and ionic liquids [EMIM][OTF] were added together in a tube. The weight ratios of the pure elastomer precursor and [EMIM][OTF] were set as 1 : 0.25, 1 : 0.5, 1 : 1, 1 : 1.5, and 1 : 2.3, yielding an IL weight ratio of 20%, 33%, 50%, 60%, and 70%, respectively. For pure PEG BBE w/o the ionic liquids, the weight ratio is 1 : 0 (IL weight ratio: 0%). The solutions were mixed by the vortex mixer with a speed of 3000 rpm for 4 minutes and used as the ionogel precursor. The ionogels were prepared by curing the ionogel precursor in the Teflon mould at 80 °C under N_2 overnight. In this work, the choice of monomers influenced the resulting polymer network structures of the elastomers. For instance, monomer EG-1 was used to form the linear elastomer. Specifically, for the preparation of PEG/IL BBIs, PEG-9 was used as the monomer.

4.4. Mechanical testing

The cyclic uniaxial tensile test was measured with a customized tensile test machine (with a 0.2 N load cell, S100 strain measurement devices). The ISO 37 – Type 4 standard was used to determine the size of the BBE sample. The BBEs or BBIs were molded into a dumb-bell test piece, with 2 mm width of narrow portion, 12 mm length of narrow portion, and 6 mm width of ends. The strain rate was set to be 0.070 s^{-1} (rate of deformation: 50 mm min^{-1}). Each sample was subjected to 10 repeated stretching-releasing cycles at the strain of 100%. The fitted

Young's modulus (E, presented in the main text and all figures) of the PEG/IL bottlebrush ionogels was determined by the fitting model in the ESI.† The engineering Young's modulus (E_{eng}) was determined by linear fitting the nominal stress–strain curve at the strain range of 0–10%.

The adhesion shear strength of the PEG/IL BBIs (IL weight ratio of 0%, 50%, and 60%) was tested by the standard lap-shear test with the same tensile test machine. The stiff thin film was adhered to the sample by cyanoacrylate glue (Krazy Glue) and used as the rigid backing for the BBIs. The adhesion area of the materials has a width of 13.8 mm and a length of 10 mm. The deformation rate of the tensile test machine was 50 mm min^{-1}. The lap shear test was stopped until the BBI sample was fully detached from the substrate materials (glass, PDMS, leaf, and wood). The shear strength was determined by dividing the maximum force by the adhesion area.

4.5. Conductivity and resistance testing

The conductivity of PEG/IL BBIs was measured by a customized four-point probe connected using a source meter (Keithley 2614B, Keithley Instrument Inc.). To reduce the contact resistance at the interface of the probes and BBI surface, the composite of Ag flakes and liquid metal EGaIn (10 wt% Ag flakes and 90 wt% EGaIn) was applied on the tip of the probes. To measure the electrical response of the PEG/IL BBIs during stretching, samples with the dimensions of 37.6 mm × 13.8 mm × 2 mm (length × width × thickness) were placed on the tensile test machine. The two ends of the sample were applied by the Ag/EGaIn composite and connected with the source meter through platinum wires to measure the resistance of the sample. The resistance change of the PEG/IL BBIs was recorded at different strains (0–100%).

4.6. Electrochemical impedance spectroscopy analysis

The AC-impedance spectra of the PEG/IL BBIs were conducted on samples with the dimension of 37.6 mm × 13.8 mm × 2 mm (length × width × thickness) through an electrochemical workstation (Autolab PGSTAT302N, Metrohm). The testing frequency ranges from 10^5 Hz to 0.1 Hz. The measuring sinusoid amplitude was 10 mV with no bias applied. The composite of Ag flakes and liquid metal EGaIn was used at the interface of BBI surfaces and probes of the electrochemical station to reduce the contact resistance.

4.7. Physical movements recording for the silkworm

To apply the PEG/IL BBI as the wearable electronics on the silkworm, the weight ratio of 1 : 1.5 was selected to ensure the worm-matched softness. The dimension of the sample was 37.6 mm × 4 mm × 1 mm (length × width × thickness). The BBI sample was attached to the back of the silkworm based on the self-adhesion property. At the two ends of the BBI sample, the composite of Ag flakes and liquid metal EGaIn was applied at the interface of platinum wires and the BBI surface to ensure a good electrical connection for the platinum wires. Two platinum wires were used to connect the BBI sample to the source meter to measure the resistance response of the BBI when the silkworm was crawling. A camera was used to record the physical movements of the silkworm.

4.8. Signal recording and electrical stimulation of the Venus flytrap

The PEG/IL BBI with an IL weight ratio of 60% was molded into circular electrodes (8 mm in diameter and 1 mm in thickness). Two pairs of PEG/IL BBI electrodes were attached to the Venus flytrap by the self-adhesion property. One pair of signal recording electrodes was attached to one lobe of the Venus flytrap and the other pair of electrical stimulation electrodes was attached to the other lobe of the Venus flytrap. For each pair of the electrodes, the positive terminal was attached to the midrib and the negative one was attached to the center of the lobe. The top surface of the electrodes was applied by the Ag/EGaIn composite and then connected with platinum wires as connectors to the source meter and power supply. The pair of signal recording electrodes was connected to the source meter. The output voltage from the Venus flytrap was recorded by the source meter. The pair of electrical stimulation electrodes was connected to the power supply to provide DC voltage of 2 V, 3 V, 4 V, and 5 V. For AC voltage supply, the pair of electrical stimulation electrodes was connected with the functional generator to provide 4 V square waves with frequencies of 1 Hz and 2 Hz. A camera was used to record the closing process of the Venus trap.

4.9. ECG recording

The PEG/IL BBI electrodes were prepared into circular electrodes (diameter × thickness: 8 mm × 2 mm). The electrodes were coated with a thin layer of Ag/EGaIn to reduce the contact resistance between PEG/IL BBI and external wires. Three PEG/IL BBI electrodes were attached to the right arm position, left arm position, and right leg position of a human chest. The external wires were then connected to the commercial ECG monitor chip (AD8232). An Arduino microcontroller (Arduino Mega) was used to power the chip and record the signal output from the chip. The Arduino was serially connected with Python, which was used to filter and save the real-time ECG signal. As a comparison, three commercial hydrogel electrodes on the Ag/AgCl were used on the human chest in the same manner to record ECG. The participants were authors of this paper, and consent was obtained from research participants before conducting the experiments.

Author contributions

P. Xu, S. Challa, P. Pan, and X. Liu designed the experiments, prepared the figures, and wrote the manuscript. P. Xu and S. Challa prepared all the materials, performed material characterizations, and conducted demonstrations. Z. Zhang, X. Wu and S. Wang provided assistance on the material characterization methods, demonstrations, and figure preparations.

Conflicts of interest

The authors declare no competing interest for this work.

Data availability

All of the data in this work are presented in the main text and the ESI.†

Acknowledgements

The authors acknowledge the financial support provided by the Natural Sciences and Engineering Research Council of Canada (grant number: RGPIN-2022-05039), Canada Foundation for Innovation (grant number: JELF-38428), and the University of Toronto (through an XSeed grant). The authors also thank Prof. Helen Tran and Angela Lin. This work stemmed from an initial collaboration with Prof. Helen Tran and she provided initial guidance during our joint research meetings.

References

1 T. Someya, Z. Bao and G. G. Malliaras, The Rise of Plastic Bioelectronics, *Nature*, 2016, **540**(7633), 379–385, DOI: 10.1038/nature21004.
2 C. Wang, C. Wang, Z. Huang and S. Xu, Materials and Structures toward Soft Electronics, *Adv. Mater.*, 2018, **30**(50), 1–49, DOI: 10.1002/adma.201801368.
3 A. Lin, A. Uva, J. Babi and H. Tran, Materials Design for Resilience in the Biointegration of Electronics, *MRS Bull.*, 2021, **46**(9), 860–869, DOI: 10.1557/s43577-021-00174-5.
4 R. C. Webb, A. P. Bonifas, A. Behnaz, Y. Zhang, K. J. Yu, H. Cheng, M. Shi, Z. Bian, Z. Liu, Y. S. Kim, W. H. Yeo, J. S. Park, J. Song, Y. Li, Y. Huang, A. M. Gorbach and J. A. Rogers, Ultrathin Conformal Devices for Precise and Continuous Thermal Characterization of Human Skin, *Nat. Mater.*, 2013, **12**, 938–944, DOI: 10.1038/nmat3755.
5 J. Lee, K. H. Ku, C. H. Park, Y. J. Lee, H. Yun and B. J. Kim, Shape and Color Switchable Block Copolymer Particles by Temperature and PH Dual Responses, *ACS Nano*, 2019, **13**(4), 4230–4237, DOI: 10.1021/acsnano.8b09276.
6 P. Xu, S. Wang, A. Lin, H.-K. Min, Z. Zhou, W. Dou, Y. Sun, X. Huang, H. Tran and X. Liu, Conductive and Elastic Bottlebrush Elastomers for Ultrasoft Electronics, *Nat. Commun.*, 2023, **14**, 623, DOI: 10.1038/s41467-023-36214-8.
7 Y. Li, N. Li, W. Liu, A. Prominski, S. Kang, Y. Dai, Y. Liu, H. Hu, S. Wai, S. Dai, Z. Cheng, Q. Su, P. Cheng, C. Wei, L. Jin, J. A. Hubbell, B. Tian and S. Wang, Achieving Tissue-Level Softness on Stretchable Electronics through a Generalizable Soft Interlayer Design, *Nat. Commun.*, 2023, **14**, 4488, DOI: 10.1038/s41467-023-40191-3.
8 C. F. Guimarães, L. Gasperini, A. P. Marques and R. L. Reis, The Stiffness of Living Tissues and Its Implications for Tissue Engineering, *Nat. Rev. Mater.*, 2020, **5**(5), 351–370, DOI: 10.1038/s41578-019-0169-1.
9 N. R. Sinatra, C. B. Teeple, D. M. Vogt, K. K. Parker, D. F. Gruber and R. J. Wood, Ultragentle Manipulation of Delicate Structures Using a Soft Robotic Gripper, *Sci. Robot.*, 2019, **4**(33), 1–12, DOI: 10.1126/SCIROBOTICS.AAX5425.
10 Y. Ohm, C. Pan, M. J. Ford, X. Huang, J. Liao and C. Majidi, An Electrically Conductive Silver–Polyacrylamide–Alginate Hydrogel Composite for Soft Electronics, *Nat. Electron.*, 2021, **4**(3), 185–192, DOI: 10.1038/s41928-021-00545-5.
11 C. M. Tringides, N. Vachicouras, I. de Lázaro, H. Wang, A. Trouillet, B. R. Seo, A. Elosegui-Artola, F. Fallegger, Y. Shin, C. Casiraghi, K. Kostarelos, S. P. Lacour and D. J. Mooney, Viscoelastic Surface Electrode Arrays to Interface with Viscoelastic Tissues, *Nat. Nanotechnol.*, 2021, **16**, 1019–1029, DOI: 10.1038/s41565-021-00926-z.
12 H. Yuk, B. Lu, S. Lin, K. Qu, J. Xu, J. Luo and X. Zhao, 3D Printing of Conducting Polymers, *Nat. Commun.*, 2020, **11**(1), 4–11, DOI: 10.1038/s41467-020-15316-7.
13 T. Zhou, H. Yuk, F. Hu, J. Wu, F. Tian, H. Roh, Z. Shen, G. Gu, J. Xu, B. Lu and X. Zhao, 3D Printable High-Performance Conducting Polymer Hydrogel for All-Hydrogel Bioelectronic Interfaces, *Nat. Mater.*, 2023, **July**, 22, DOI: 10.1038/s41563-023-01569-2.
14 V. R. Feig, H. Tran, M. Lee and Z. Bao, Mechanically Tunable Conductive Interpenetrating Network Hydrogels That Mimic the Elastic Moduli of Biological Tissue, *Nat. Commun.*, 2018, **9**(1), 1–9, DOI: 10.1038/s41467-018-05222-4.
15 Y. Liu, J. Li, S. Song, J. Kang, Y. Tsao, S. Chen, V. Mottini, K. McConnell, W. Xu, Y. Q. Zheng, J. B. H. Tok, P. M. George and Z. Bao, Morphing Electronics Enable Neuromodulation in Growing Tissue, *Nat. Biotechnol.*, 2020, **38**, 1031–1036, DOI: 10.1038/s41587-020-0495-2.
16 H. Yuk, T. Zhang, G. A. Parada, X. Liu and X. Zhao, Skin-Inspired Hydrogel-Elastomer Hybrids with Robust Interfaces and Functional Microstructures, *Nat. Commun.*, 2016, **7**, 1–11, DOI: 10.1038/ncomms12028.
17 H. J. Kim, B. Chen, Z. Suo and R. C. Hayward, Ionoelastomer Junctions between Polymer Networ of Fixed Anions and Cations, *Science*, 2020, **367**(6479), 773–776, DOI: 10.1126/science.aay8467.
18 J. L. Self, V. G. Reynolds, J. Blankenship, E. Mee, J. Guo, K. Albanese, R. Xie, C. J. Hawker, J. R. de Alaniz, M. L. Chabinyc and C. M. Bates, Carbon Nanotube Composites with Bottlebrush Elastomers for Compliant Electrodes, *ACS Polym. Au*, 2022, **2**(1), 27–34, DOI: 10.1021/acspolymersau.1c00034.
19 M. Vatankhah-Varnosfaderani, W. F. M. Daniel, M. H. Everhart, A. A. Pandya, H. Liang, K. Matyjaszewski, A. V. Dobrynin and S. S. Sheiko, Mimicking Biological Stress–Strain Behaviour with Synthetic Elastomers, *Nature*, 2017, **549**(7673), 497–501, DOI: 10.1038/nature23673.
20 W. F. M. Daniel, J. Burdyńska, M. Vatankhah-Varnoosfaderani, K. Matyjaszewski, J. Paturej, M. Rubinstein, A. V. Dobrynin and S. S. Sheiko, Solvent-Free, Supersoft and Superelastic Bottlebrush Melts and Networks, *Nat. Mater.*, 2016, **15**(2), 183–189, DOI: 10.1038/nmat4508.
21 L. H. Cai, T. E. Kodger, R. E. Guerra, A. F. Pegoraro, M. Rubinstein and D. A. Weitz, Soft Poly(Dimethylsiloxane) Elastomers from Architecture-Driven Entanglement Free Design, *Adv. Mater.*, 2015, **27**(35), 5132–5140, DOI: 10.1002/adma.201502771.

22 A. N. Keith, M. Vatankhah-Varnosfaderani, C. Clair, F. Fahimipour, E. Dashtimoghadam, A. Lallam, M. Sztucki, D. A. Ivanov, H. Liang, A. V. Dobrynin and S. S. Sheiko, Bottlebrush Bridge between Soft Gels and Firm Tissues, *ACS Cent. Sci.*, 2020, **6**(3), 413–419, DOI: **10.1021/acscentsci.9b01216**.

23 V. G. Reynolds, S. Mukherjee, R. Xie, A. E. Levi, A. Atassi, T. Uchiyama, H. Wang, M. L. Chabinyc and C. M. Bates, Super-Soft Solvent-Free Bottlebrush Elastomers for Touch Sensing, *Mater. Horiz.*, 2020, **7**(1), 181–187, DOI: **10.1039/c9mh00951e**.

24 P. Hu, J. Madsen and A. L. Skov, One Reaction to Make Highly Stretchable or Extremely Soft Silicone Elastomers from Easily Available Materials, *Nat. Commun.*, 2021, **18**, 370, DOI: **10.1038/s41467-022-28015-2**.

25 Z. Zhao, G. D. Spyropoulos, C. Cea, J. N. Gelinas and D. Khodagholy, Ionic Communication for Implantable Bioelectronics, *Sci. Adv.*, 2022, **8**(14), 1–12, DOI: **10.1126/sciadv.abm7851**.

26 L. Yang, L. Gan, Z. Zhang, Z. Zhang, H. Yang, Y. Zhang and J. Wu, Insight into the Contact Impedance between the Electrode and the Skin Surface for Electrophysical Recordings, *ACS Omega*, 2022, **7**(16), 13906–13912, DOI: **10.1021/acsomega.2c00282**.

27 J. Rivnay, R. M. Owens and G. G. Malliaras, The Rise of Organic Bioelectronics, *Chem. Mater.*, 2014, **26**(1), 679–685, DOI: **10.1021/cm4022003**.

28 S. Inal, J. Rivnay, A. O. Suiu, G. G. Malliaras and I. McCulloch, Conjugated Polymers in Bioelectronics, *Acc. Chem. Res.*, 2018, **51**(6), 1368–1376, DOI: **10.1021/acs.accounts.7b00624**.

29 S. Koneshan, J. C. Rasaiah, R. M. Lynden-Bell and S. H. Lee, Solvent Structure, Dynamics, and Ion Mobility in Aqueous Solutions at 25 °C, *J. Phys. Chem. B*, 1998, **102**(21), 4193–4204, DOI: **10.1021/jp980642x**.

30 Y. Wang, H. Liu, H. Xie and S. Zhou, An Autofluorescent Hydrogel with Water-Dependent Emission for Dehydration-Visualizable Smart Wearable Electronics, *Adv. Funct. Mater.*, 2023, **33**(19), 2213545, DOI: **10.1002/adfm.202213545**.

31 J. S. Wilkes, A Short History of Ionic Liquids - From Molten Salts to Neoteric Solvents, *Green Chem.*, 2002, **4**(2), 73–80, DOI: **10.1039/b110838g**.

32 J. D. Holbrey and K. R. Seddon, Ionic Liquids, *Clean Technol. Environ. Policy*, 1999, **1**(4), 223–236, DOI: **10.1007/s10098005003 6**.

33 M. C. Buzzeo, R. G. Evans and R. G. Compton, Non-Haloaluminate Room-Temperature Ionic Liquids in Electrochemistry – A Review, *ChemPhysChem*, 2004, **5**(8), 1106–1120, DOI: **10.1002/cphc.200301017**.

34 Y. Ding, J. Zhang, L. Chang, X. Zhang, H. Liu and L. Jiang, Preparation of High-Performance Ionogels with Excellent Transparency, Good Mechanical Strength, and High Conductivity, *Adv. Mater.*, 2017, **29**(47), 1–7, DOI: **10.1002/adma.201704253**.

35 X. Xiao, M. Wang, S. Chen, Y. Zhang, H. Gu, Y. Deng, G. Yang, C. Fei, B. Chen, Y. Lin, M. D. Dickey and J. Huang, Lead-Adsorbing Ionogel-Based Encapsulation for Impact-Resistant, Stable, and Lead-Safe Perovskite Modules, *Sci. Adv.*, 2021, **7**(44), 1–10, DOI: **10.1126/sciadv.abi8249**.

36 Y. Ren, J. Guo, Z. Liu, Z. Sun, Y. Wu, L. Liu and F. Yan, Ionic Liquid – Based Click-Ionogels, *Sci. Adv.*, 2019, **5**(8), eaax0648.

37 A. P. S. Brogan, C. J. Clarke, A. Charalambidou, C. N. Loynachan, S. E. Norman, J. Doutch and J. P. Hallett, Expanding the Design Space of Gel Materials through Ionic Liquid Mediated Mechanical and Structural Tuneability, *Mater. Horiz.*, 2020, **7**(3), 820–826, DOI: **10.1039/c9mh01496a**.

38 O. Vassiliadou, V. Chrysostomou, S. Pispas, P. A. Klonos and A. Kyritsis, Molecular Dynamics and Crystallization in Polymers Based on Ethylene Glycol Methacrylates (EGMAs) with Melt Memory Characteristics: From Linear Oligomers to Comb-like Polymers, *Soft Matter*, 2021, **17**(5), 1284–1298, DOI: **10.1039/d0sm01666g**.

39 A. R. Choudhury, N. Winterton, A. Steiner, A. I. Cooper and K. A. Johnson, In Situ Crystallization of Ionic Liquids with Melting Points below −25 °C, *CrystEngComm*, 2006, **8**(10), 742–745, DOI: **10.1039/b609598d**.

40 A. Hailu and S. K. Shaw, Efficient Electrocatalytic Reduction of Carbon Dioxide in 1-Ethyl-3-Methylimidazolium Trifluoromethanesulfonate and Water Mixtures, *Energy Fuels*, 2018, **32**(12), 12695–12702, DOI: **10.1021/acs.energyfuels.8b02750**.

41 M. Musiał, E. Zorebski, K. Malarz, M. Kuczak, A. Mrozek-Wilczkiewicz, J. Jacquemin and M. Dzida, Cytotoxicity of Ionic Liquids on Normal Human Dermal Fibroblasts in the Context of Their Present and Future Applications, *ACS Sustainable Chem. Eng.*, 2021, **9**(22), 7649–7657, DOI: **10.1021/acssuschemeng.1c02277**.

42 J. Li, S. Ji, X. Yu, X. Yuan, K. Zhang and L. Ren, Magnetic Poly(Ionic Liquid)s: Bottlebrush versus Linear Structures, *Macromolecules*, 2022, **55**(6), 2067–2074, DOI: **10.1021/acs.macromol.1c02457**.

43 Z. Q. Lu, Z. Yin, L. L. Zhang, Y. Yan, Z. Jiang, H. Wu and W. Wang, Synthesis of Proton Conductive Copolymers of Inorganic Polyacid Cluster Polyelectrolytes and PEO Bottlebrush Polymers, *Macromolecules*, 2022, **55**(8), 3301–3310, DOI: **10.1021/acs.macromol.1c02443**.

44 X. Liu and P. M. Claesson, Bioinspired Bottlebrush Polymers for Aqueous Boundary Lubrication, *Polymers*, 2022, **14**(13), 1–17, DOI: **10.3390/polym14132724**.

45 S. Mukherjee, R. Xie, V. G. Reynolds, T. Uchiyama, A. E. Levi, E. Valois, H. Wang, M. L. Chabinyc and C. M. Bates, Universal Approach to Photo-Crosslink Bottlebrush Polymers, *Macromolecules*, 2020, **53**(3), 1090–1097, DOI: **10.1021/acs.macromol.9b02210**.

46 N. Markovic, N. K. Dutta, D. R. Williams and J. Matisons, Solvent Effects on the Kinetics of Gelation and the Crosslink Density of Polysiloxane Gels, *Silicon Chem.*, 2005, **2**(5–6), 223–233, DOI: **10.1007/s11201-005-4579-0**.

47 L. A. Idowu and R. A. Hutchinson, Solvent Effects on Radical Copolymerization Kinetics of 2-Hydroxyethyl Methacrylate

and Butyl Methacrylate, *Polymers*, 2019, **11**(3), 487, DOI: 10.3390/polym11030487.

48 M. Akhmanova, E. Osidak, S. Domogatsky, S. Rodin and A. Domogatskaya, Physical, Spatial, and Molecular Aspects of Extracellular Matrix of in Vivo Niches and Artificial Scaffolds Relevant to Stem Cells Research, *Stem Cells Int.*, 2015, **2015**, 167025, DOI: 10.1155/2015/167025.

49 O. Chaudhuri, J. Cooper-White, P. A. Janmey, D. J. Mooney and V. B. Shenoy, Effects of Extracellular Matrix Viscoelasticity on Cellular Behaviour, *Nature*, 2020, **584**(7822), 535–546, DOI: 10.1038/s41586-020-2612-2.

50 R. Verduzco, X. Li, S. L. Pesek and G. E. Stein, Structure, Function, Self-Assembly, and Applications of Bottlebrush Copolymers, *Chem. Soc. Rev.*, 2015, **44**(8), 2405–2420, DOI: 10.1039/c4cs00329b.

51 Z. Cao, W. F. M. Daniel, M. Vatankhah-Varnosfaderani, S. S. Sheiko and A. V. Dobrynin, Dynamics of Bottlebrush Networks, *Macromolecules*, 2016, **49**(20), 8009–8017, DOI: 10.1021/acs.macromol.6b01358.

52 N. M. Barkoula, B. Alcock, N. O. Cabrera and T. Peijs, An Investigation on the Rheology, Morphology, Thermal and Mechanical Properties of Recycled Poly(Ethylene Terephthalate) Reinforced With Modified Short Glass Fibers, *Polym. Compos.*, 2009, **30**(7), 993–999, DOI: 10.1002/pc.20647.

53 J. L. Self, V. G. Reynolds, J. Blankenship, E. Mee, J. Guo, K. Albanese, R. Xie, C. J. Hawker, J. R. de Alaniz, M. L. Chabinyc and C. M. Bates, Carbon Nanotube Composites with Bottlebrush Elastomers for Compliant Electrodes, *ACS Polym. Au*, 2021, **2**(1), 27–34, DOI: 10.1021/acspolymersau.1c00034.

54 I. Chodák, M. Omastová and J. Pionteck, Relation between Electrical and Mechanical Properties of Conducting Polymer Composites, *J. Appl. Polym. Sci.*, 2001, **82**(8), 1903–1906, DOI: 10.1002/app.2035.

55 K. Watanabe, *Active dissolution mechanisms of iron using EIS WITH channel flow double electrode. Influences of chloride and fluoride ions*, 1996, vol. 41.

56 C. J. Wang, F. Vashahi, I. Moutsios, A. Z. Umarov, G. G. Ageev, Z. Wang, D. A. Ivanov, A. V. Dobrynin and S. S. Sheiko, Bottlebrush Hydrogels with Hidden Length: Super-Swelling and Mechanically Robust, *Adv. Funct. Mater.*, 2024, **2410905**, 1–9, DOI: 10.1002/adfm.202410905.

57 F. Vashahi, M. R. Martinez, E. Dashtimoghadam, F. Fahimipour, A. N. Keith, E. A. Bersenev, D. A. Ivanov, E. B. Zhulina, P. Popryadukhin, K. Matyjaszewski, M. Vatankhah-Varnosfaderani and S. S. Sheiko, Injectable Bottlebrush Hydrogels with Tissue-Mimetic Mechanical Properties, *Sci. Adv.*, 2022, **8**(3), 1–12, DOI: 10.1126/sciadv.abm2469.

58 C. Yang, M. W. Tibbitt, L. Basta and K. S. Anseth, Mechanical Memory and Dosing Influence Stem Cell Fate, *Nat. Mater.*, 2014, **13**(6), 645–652, DOI: 10.1038/nmat3889.

59 M. Maw, E. Dashtimoghadam, A. N. Keith, B. J. Morgan, A. K. Tanas, E. Nikitina, D. A. Ivanov, M. Vatankhah-Varnosfaderani, A. V. Dobrynin and S. S. Sheiko, Sticky Architecture: Encoding Pressure Sensitive Adhesion in Polymer Networks, *ACS Cent. Sci.*, 2022, **9**(2), 197–205, DOI: 10.1021/acscentsci.2c01407.

60 A. Vioux, L. Viau, S. Volland and J. Le Bideau, Use of Ionic Liquids in Sol–Gel; Ionogels and Applications, *C. R. Chim.*, 2010, **13**(1–2), 242–255, DOI: 10.1016/j.crci.2009.07.002.

61 A. L. Dorfmann, W. A. Woods and B. A. Trimmer, Muscle Performance in a Soft-Bodied Terrestrial Crawler: Constitutive Modelling of Strain-Rate Dependency, *J. R. Soc., Interface*, 2008, **5**(20), 349–362, DOI: 10.1098/rsif.2007.1076.

62 B. A. Trimmer and H. T. Lin, Bone-Free: Soft Mechanics for Adaptive Locomotion, *Integr. Comp. Biol.*, 2014, **54**(6), 1122–1135, DOI: 10.1093/icb/icu076.

63 T. Umedachi, M. Shimizu and Y. Kawahara, Caterpillar-Inspired Crawling Robot Using Both Compression and Bending Deformations, *IEEE Robot. Autom. Lett.*, 2019, **4**(2), 670–676, DOI: 10.1109/LRA.2019.2893438.

64 S. Lee, S. Franklin, F. A. Hassani, T. Yokota, M. O. G. Nayeem, Y. Wang, R. Leib, G. Cheng, D. W. Franklin and T. Someya, Nanomesh Pressure Sensor for Monitoring Finger Manipulation without Sensory Interference, *Science*, 2020, **370**(6519), 966–970, DOI: 10.1126/science.abc9735.

65 C. Appiah, C. Arndt, K. Siemsen, A. Heitmann, A. Staubitz and C. Selhuber-Unkel, Living Materials Herald a New Era in Soft Robotics, *Adv. Mater.*, 2019, **31**(36), 1807747, DOI: 10.1002/adma.201807747.

66 C. Yang and Z. Suo, Hydrogel Ionotronics, *Nat. Rev. Mater.*, 2018, **3**(6), 125–142, DOI: 10.1038/s41578-018-0018-7.

67 W. Li, N. Matsuhisa, Z. Liu, M. Wang, Y. Luo, P. Cai, G. Chen, F. Zhang, C. Li, Z. Liu, Z. Lv, W. Zhang and X. Chen, An On-Demand Plant-Based Actuator Created Using Conformable Electrodes, *Nat. Electron.*, 2021, **4**(2), 134–142, DOI: 10.1038/s41928-020-00530-4.

68 A. G. Volkov, J. C. Foster, T. A. Ashby, R. K. Walker, J. A. Johnson and V. S. Markin, Mimosa Pudica: Electrical and Mechanical Stimulation of Plant Movements, *Plant, Cell Environ.*, 2010, **33**(2), 163–173, DOI: 10.1111/j.1365-3040.2009.02066.x.

69 X. Yan, Z. Wang, L. Huang, C. Wang, R. Hou, Z. Xu and X. Qiao, Research Progress on Electrical Signals in Higher Plants, *Prog. Nat. Sci.*, 2009, **19**(5), 531–541, DOI: 10.1016/j.pnsc.2008.08.009.

70 Y. Liu, J. Liu, S. Chen, T. Lei, Y. Kim, S. Niu, H. Wang, X. Wang, A. M. Foudeh, J. B. H. Tok and Z. Bao, Soft and Elastic Hydrogel-Based Microelectronics for Localized Low-Voltage Neuromodulation, *Nat. Biomed. Eng.*, 2019, **3**(1), 58–68, DOI: 10.1038/s41551-018-0335-6.

71 E. Axpe, G. Orive, K. Franze and E. A. Appel, Towards Brain-Tissue-like Biomaterials, *Nat. Commun.*, 2020, **11**(1), 10–13, DOI: 10.1038/s41467-020-17245-x.

